TRAJAN

Trajan Scientific and Medical

Modelling and experimental progress towards the fabrication of robust constant-bore emitters and their evaluation on a novel electrospray test device.

Kyle Bachus[1]; Joe Giddings[2]; Herbert Foo[1]; Heike Ebendorff-Heidepriem[2, 3]; Yvonne Stokes[2]; Andrew Gooley[1]
1) Trajan Scientific and Medical, Ringwood, Australia
2) University of Adelaide, Adelaide, Australia
3) Institute for Photonics and Advanced Sensing, Adelaide, Australia

Electrospray introduction

The electrospray process

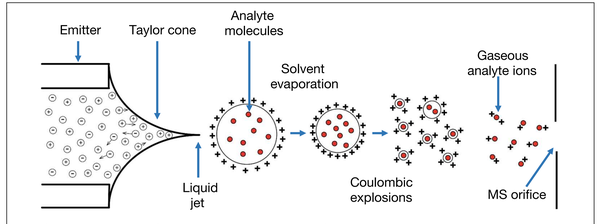

Figure 1. Schematic illustration of typical ESI process and formation of gas phase ions for MS analysis.

nanoESI and multi-ESI

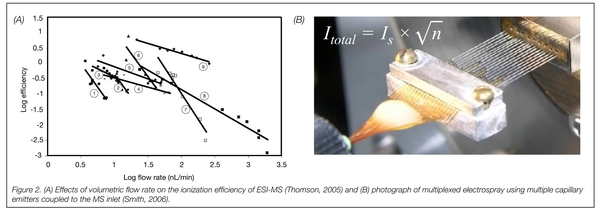

Figure 2. (A) Effects of volumetric flow rate on the ionization efficiency of ESI-MS (Thomson, 2005) and (B) photograph of multiplexed electrospray using multiple capillary emitters coupled to the MS inlet (Smith, 2006).

- Lower volumetric flow rates generates smaller droplets at the onset of ESI.
- Smaller droplets lead to more efficient ionization and improved surface charge.
- Overall improvement in workflow sensitivity.
- Splits convenient µ-flow into nano flow regime.
- Reduces the effects of potential clogging.
- Significant increase in theoretical ion flux.
- Overall improvement in workflow sensitivity.

Constant ID versus tapered ID emitter tips

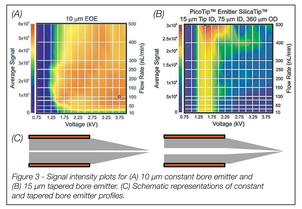

Figure 3 - Signal intensity plots for (A) 10 µm constant bore emitter and (B) 15 µm tapered bore emitter. (C) Schematic representations of constant and tapered bore emitter profiles.

- Constant ID dramatically reduces propensity for clogging, making them more effective and robust for biological analyses.
- Smaller IDs can be achieved by tapering and can therefore improve ionization efficiency.
- Tapered ID tends to limit the dynamic range of flow rate and applied voltage within the workflow as discussed by Timperman et al.
- There is a lack of emitter tips currently available that can leverage narrow ID (<10 µm) without tapering the inner bore.

TR-MS02-C Date date of Trajan Scientific Australia Pty Ltd 2020

Hydrofluoric acid etching

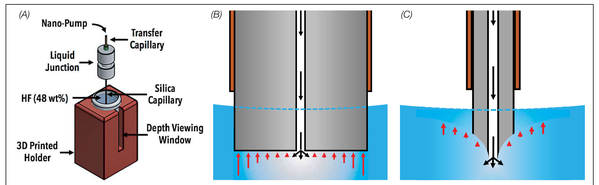

Figure 4. (A) Schematic representation of the wet-chemical etching method showing the capillary submerged into a solution of HF (48 wt%); (B) and (C) show schematic representations of the gradient in [HF] generated by fluid flowing through the bore of the capillary and the respective (B) initial and (C) final profiles.

- The etching protocol and capillary embodiment can be multiplexed using micro structured fibre technology to form multi-lumen ESI emitters.
- Borosilicate glass can be introduced into the quartz via spatial control to inflict differential etch rates along the cross section of the fibre.
- These differential etch rates can be exploited to develop specific structures at the facet.

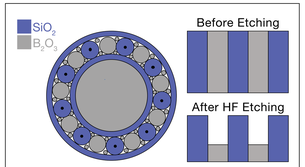

Figure 5. Schematic diagrams of (Left) the preform design and (Right) the differential etch rates between B_2O_3 (grey) and fused silica (blue).

Modelling and simulations

Establishing the etch rate: Beyond theoretical

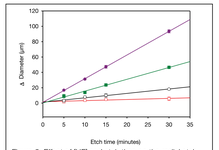

Figure 6. Effect of [HF] and etch time on the radial etch rates of fused-silica tubing.

- OD measurements before and after etching a 360 µm capillary in various [HF] provide the necessary data for determining the native etch rates of fused silica tubing as a function of [HF].
- Observed etch rates were commensurate with previous studies performed under similar conditions on quartz materials.
- The native etch rate can then be built into a mathematical model to better understand the effects fluid flow through the bore on the localized etch rates.

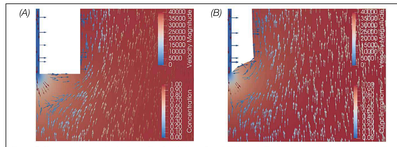

Parameter	Value	Units
ρ_a	1.15×10^3	kg/m^3
ρ_w	1.00×10^3	kg/m^3
ρ_i	2.65×10^3	kg/m^3
μ	0.9	mPa·s
r_a	2-5	µm
$\bar{R}$	62.5	µm
k_f	7.639 - 7.692	nm/s
k_s	2.475 - 2.560	
$\bar{Q}$	1- 200	nL/min
$\bar{D}$	1- 20	nm^2/s

Figure 7. Concentration and velocity profiles for (A) time=0 and (B) time=t. The background colour represents the concentration of acid and the arrows represent dimensionless velocity and the direction of flow in the acid.

Parametric modelling results

Flow rate

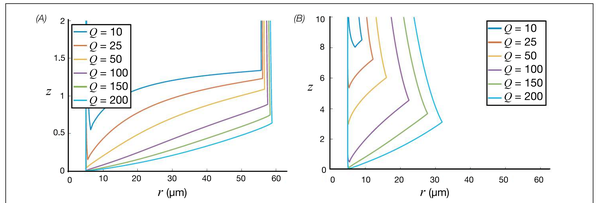

Figure 8. Simulated emitter profiles with constant fluid diffusivity (D = 10) and variable flow rates at (A) t = 3 minutes and (B) time = 25 minutes.

Diffusivity

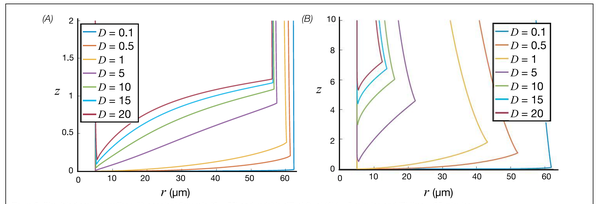

Figure 9. Simulated emitter profiles with constant flow rate (Q = 50) and variable diffusivity at (A) t = 3 minutes and (B) time = 25 minutes.

Experimental results

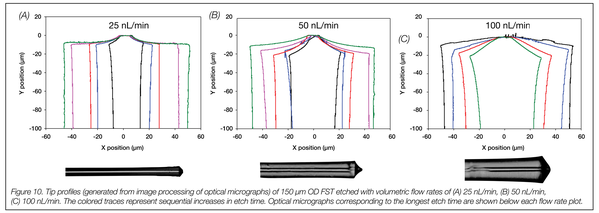

Figure 10. Tip profiles (generated from image processing of optical micrographs) of 150 µm OD FST etched with volumetric flow rates of (A) 25 nL/min, (B) 50 nL/min, (C) 100 nL/min. The colored traces represent sequential increases in etch time. Optical micrographs corresponding to the longest etch time are shown below each flow rate plot.

- Simulated profiles suggest that volumetric flow rate and diffusivity of the fluid dominate the etching process.
- Modelling suggested and experiment confirmed that lower flow rates increases the rate of etching and generates concave tip geometries compared to shallow convex geometries at higher volumetric flow rates.
- Within a subset of flow rate, longer etch times provide a more suitable tip geometry for ESI-MS and it is expected that the resulting Taylor cone formation will provide improvements in ion flux and efficiency.

Comparative analysis

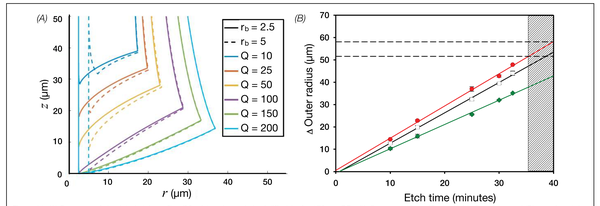

Figure 11. (A) Summary of simulated etch profiles (30 min) under optimized diffusivity for 150 µm OD with 5 µm and 10 µm ID at variable flow rates and (B) experimental data for etch rates under 25 nL/min (red), 50 nL/min (black) and 100 nL/min (green).

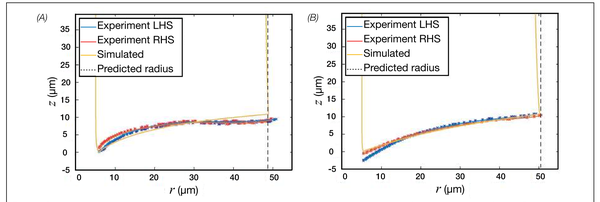

Figure 12. Comparative plots showing simulated and experimental profiles overplayed after 10 minutes of etching with volumetric flow rates of (A) Q = 25 nL/min and (B) Q = 50 nL/min.

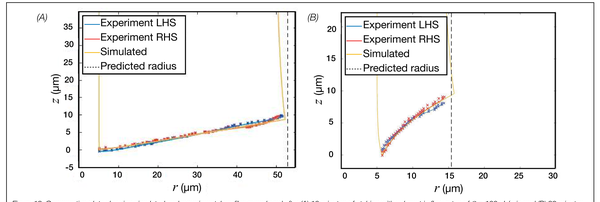

Figure 13. Comparative plots showing simulated and experimental profiles overplayed after (A) 10 minutes of etching with volumetric flow rates of Q = 100 nL/min and (B) 32 minutes of etching at Q = 25 nL/min.

Future work

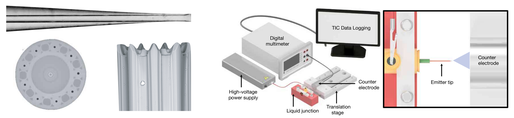

Contact info@trajanscimed.com for further information